doi:10.1016/j.jmb.2008.07.051 J. Mol. Biol. (2008) 382, 931–941

JMB

Available online at www.sciencedirect.com

ScienceDirect

ELSEVIER

The Structure of Interleukin-23 Reveals the Molecular Basis of p40 Subunit Sharing with Interleukin-12

Patrick J. Lupardus and K. Christopher Garcia*

Howard Hughes Medical Institute, Departments of Molecular and Cellular Physiology and Structural Biology, Stanford University School of Medicine, Stanford, CA 94305, USA

Received 5 June 2008; received in revised form 17 July 2008; accepted 19 July 2008
Available online 25 July 2008

Interleukin (IL)-23 is a recently identified member of the IL-12 family of heterodimeric cytokines that modulate subpopulations of T helper cells, and both IL-12 and IL-23 are attractive targets for therapy of autoimmune diseases. IL-23 is a binary complex of a four-helix bundle cytokine (p19) and a soluble class I cytokine receptor p40. IL-12 and IL-23 share p40 as an α-receptor subunit, yet show only 15% sequence homology between their four-helix cytokines p19 and p35, respectively, and signal through different combinations of shared receptors. In order to elucidate the structural basis of p40 sharing, we have determined a 2.3-Å crystal structure of IL-23 for comparison to the previously determined structure of IL-12. The docking mode of p19 to p40 is altered compared to p35, deviating by a 'tilt' and 'roll' that results in an altered footprint of p40 on the A and D helices of the respective cytokines. Binding of p19 to p40 is mediated primarily by an arginine residue on helix D of p19 that forms an extensive charge and hydrogen-bonding network with residues at the base of a pocket on p40. This 'arginine pocket' is lined with an inner shell of hydrophobic interactions that are ringed by an outer shell of polar interactions. Comparative analysis indicates that the IL-23 and IL-12 complexes 'mimic' the network of interactions constituting the central arginine pocket despite p19 and p35 having limited sequence homology. The majority of the structural epitopes in the two complexes are composed of unique p19 and p35 pairwise contacts with common residues on p40. Thus, while the critical hotspot is maintained in the two complexes, the majority of the interfaces are structurally distinct and, therefore, provide a basis for the therapeutic targeting of IL-12 *versus* IL-23 heterodimer formation despite their use of a common receptor subunit.

Edited by I. Wilson

Keywords: IL-23; IL-12; cytokine; receptor; crystallography

Introduction

The interactions of four-helix bundle cytokines with their class I cytokine receptors control many aspects of cellular development, differentiation, and proliferation across the immune, nervous, and hematopoietic systems. Engagement of cytokines by their receptors results in receptor homo- or heterodimerization, leading to the activation of intracellular Janus kinase (Jak)/signal transducer and activator of transcription (Stat) signaling cascades.[1] Four-helix bundle cytokines have a stereotypical up–up–down–down helical topology for both short- and long-chain members of the family.[2] Cytokine receptors also have several conserved features, such as the presence of a cytokine-binding homology region that is characterized by tandem fibronectin-type III (FnIII) domains containing a hallmark pattern of disulfide bonds and a WSXWS motif in the second of the FnIII domains.[3] The prototypical long-chain cytokine human growth hormone was shown to homodimerize its receptors using a 'site I/site II' paradigm through the sides of its helices, and the receptors engaged the cytokine through interstrand loops at the junction of the two FnIII domains.[4,5] While this basic building block has been found in structures of

*Corresponding author. E-mail address: kcgarcia@stanford.edu.

Abbreviations used: IL, interleukin; Jak, Janus kinase; Stat, signal transducer and activator of transcription; FnIII, fibronectin-type III; Th, T helper; GCSF, granulocyte colony-stimulating factor; PDB, Protein Data Bank.

all cytokine receptor complexes, the gp130, or interleukin (IL)-6/IL-12 family of cytokines, has evolved an additional receptor binding epitope (termed site III) that requires the presence of a top-mounted Ig domain on the receptors to homo- or heterodimerize signaling complexes in the 'tall' receptor family (e.g., gp130, LIF-R, and IL-12).[6,7] Recently, several orphan members of the IL-12 class of cytokines, IL-23 and IL-27, have been paired with their cognate receptors, and their biological activities were clarified.[8,9] In particular, IL-23 has generated a great deal of excitement with regard to its potential role in immune modulation of different subpopulations of T helper (Th) cells in concert with IL-12.[10,11]

IL-12 and IL-23 are heterodimeric cytokines that, unlike typical four-helix cytokines that are secreted alone, are secreted from dendritic cells and macrophages as disulfide-linked complexes between the helical cytokines p35 and p19, respectively (Fig. 1), and a shared binding protein termed p40.[11–14] Both p35 and p19 have sequence homology to IL-6 and granulocyte colony-stimulating factor (GCSF), marking them as members of the gp130 class of long-chain cytokines, and the p40 subunit is similar in structure to typical class I cytokine receptors such as the nonsignaling α-receptors for IL-6 and ciliary neurotrophic factor.[15] In essence, IL-12 and IL-23 represent cytokines constitutively associated with a soluble α-receptor subunit. While many cytokines exist as naturally 'shed' soluble complexes with their α-receptors,[16] IL-12 and IL-23 are unique in that they are secreted as binary complexes.

With regard to receptor activation, while IL-12 and IL-23 share p40, they signal through different heterodimeric cell surface complexes involving receptors homologous to gp130 (Fig. 1). IL-12 (p35/p40) signals through a heterodimer consisting of IL-12Rβ1 and IL-12Rβ2,[17] whereas IL-23 (p19/p40) signals through a heterodimer consisting of IL-12Rβ1 and the IL-12Rβ2-like receptor called IL-23R.[8] The architecture of the IL-12 and IL-23 receptor signaling complexes can be predicted to recapitulate features of the site I/II/III paradigm based on the organizing principles seen for other members of the tall receptor family such as gp130/IL-6, GCSF/GCSF-R, and LIF/LIF-R.[7,18] IL-23 also activates the same spectrum of Jak/Stat signaling molecules as IL-12: Jak2, Tyk2, Stat1, Stat3, Stat4, and Stat5.[8]

Biologically, it first seemed likely that these two cytokines would have redundant roles in immune homeostasis, namely, Th1-type responses that are important for cell-mediated antimicrobial and cytotoxic activities, based on their shared use of p40 as a subunit. However, it was quickly shown that their functions are nonredundant.[11] Whereas IL-12 drives the typical Th1 responses such as interferon-γ production, IL-23 does not influence the development of Th1 cells, but instead drives the development of an alternate $CD4^+$ T-cell population (now termed Th17 cells) that are notable for their production of proinflammatory IL-17 cytokines.[19] Several studies have shown that IL-23 regulation of autoreactive Th17 cells plays a critical role in the development of chronic autoimmune disorders.[20–22] Recently, IL-23 has also been shown to possess tumor-promoting proinflammatory activity and IL-23 blockade can render tumors susceptible to infiltration by IL-12-induced cytotoxic T cells.[23] These studies have led to considerable interest in the possibility of therapeutic IL-23 blockade for treatment of autoimmune disorders and, potentially, cancer.

Because IL-12 and IL-23 share their p40 subunit, it is important to delineate common *versus* cytokine-specific protein–protein interactions to serve as guideposts for the potential development of IL-12-*versus* IL-23-specific antagonists. Here, we present a structural analysis of IL-23 that represents an important benchmark in elucidating the molecular basis of p40 subunit sharing with IL-12 and in understanding the assembly of their respective

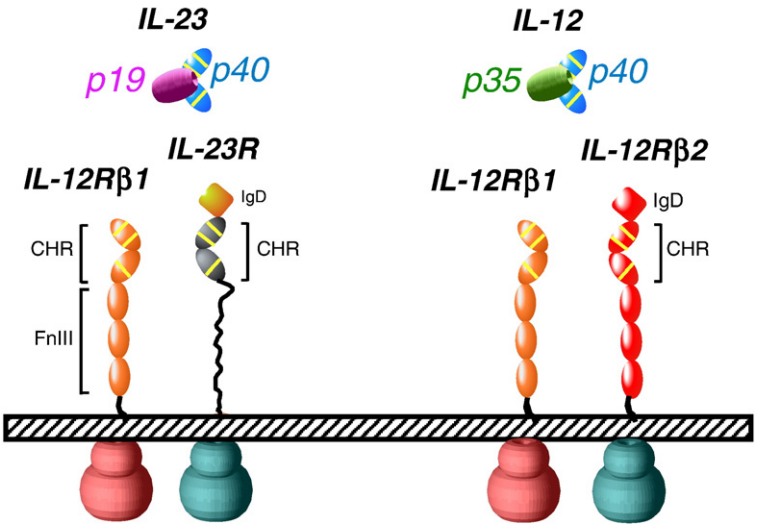

Fig. 1. Schematic representation of IL-23 and IL-12 signaling complexes. IgD stands for Ig-like domain, while CHR denotes cytokine-binding homology region and FnIII denotes fibronectin-type III domain. Yellow lines denote two conserved disulfide linkages and the conserved WSXWS motif.

Table 1. Data collection and refinement statistics for IL-23

	IL-23 native
Data collection	
Space group	*C*2
Cell dimensions	
a, *b*, *c* (Å)	116.1, 60.0, 160.4
α, β, γ (°)	90, 90.5, 90
Wavelength (Å)	0.976
Resolution (Å)	30–2.30 (2.42–2.30)
R_{merge}	0.073 (0.556)
$I/\sigma I$	13.6 (2.5)
Completeness (%)	99.9 (100.0)
Redundancy	3.7 (3.7)
Refinement	
Resolution (Å)	30–2.30
No. of reflections (total/test)	46,921/2502
R_{work}/R_{free}	0.228/0.268
No. of atoms	7016
Protein	6786
Sugar	28
Water	202
B-factors	
Protein	46.8
Sugar	56.6
Water	40.8
RMSDs	
Bond lengths (Å)	0.012
Bond angles (°)	1.527
Ramachandran plot[a] (%)	
Most favorable	87.1
Additionally allowed	12.6
Generously allowed	0.0
Disallowed	0.2

Values for the highest-resolution shell are in parentheses.
[a] Ramachandran statistics were calculated using PROCHECK.[35]

signaling complexes based on the organizing principles derived from other members of the gp130/IL-6/IL-12 family.

Results

We expressed IL-23 by coinfection of insect HiFive cells with recombinant baculoviruses carrying cDNAs for p19 and p40. The complex was purified by gel filtration as a single peak of disulfide-linked dimer (data not shown), confirming the integrity of the IL-23 heterodimer as shown for IL-12.[15] IL-23 was crystallized and the structure was determined to a resolution of 2.3 Å by molecular replacement using the coordinates of p40,[15] and p19 was then built from the partial phases in order to eliminate model bias that would be introduced by using p35 as a starting model (Table 1). During the expression, Asn-linked glycans were deglycosylated with EndoH in order to debulk the complex of carbohydrate moieties, and the surface lysines were methylated in order to grow large, well-ordered crystals. The deglycosylated and methylated IL-23 behaved identically to unmodified IL-23 during purification, while crystal diffraction was markedly improved (~4.5 to 2.3 Å).

The overall structure of IL-23 is typical of class I cytokine receptor complexes and strongly resembles the p35/p40 heterodimer structure of IL-12 (discussed below) (Fig. 2). The p40 subunit, as previously seen, is composed of three domains (D1, D2, and D3) of approximate dimensions 100×45×25 Å and superimposes with the previous human p40 structure with an overall root-mean-square deviation (RMSD) of 1.3 Å. The D1 domain is an S-type Ig fold in which strand A is swapped from the three-strand sheet so that it now joins the four-strand sheet. The D1 domain interacts with the D2 domain in an unusual fashion in which the long axis of the domain is displaced from colinearity with the D2 domain, such that it engages the top of D2 in a

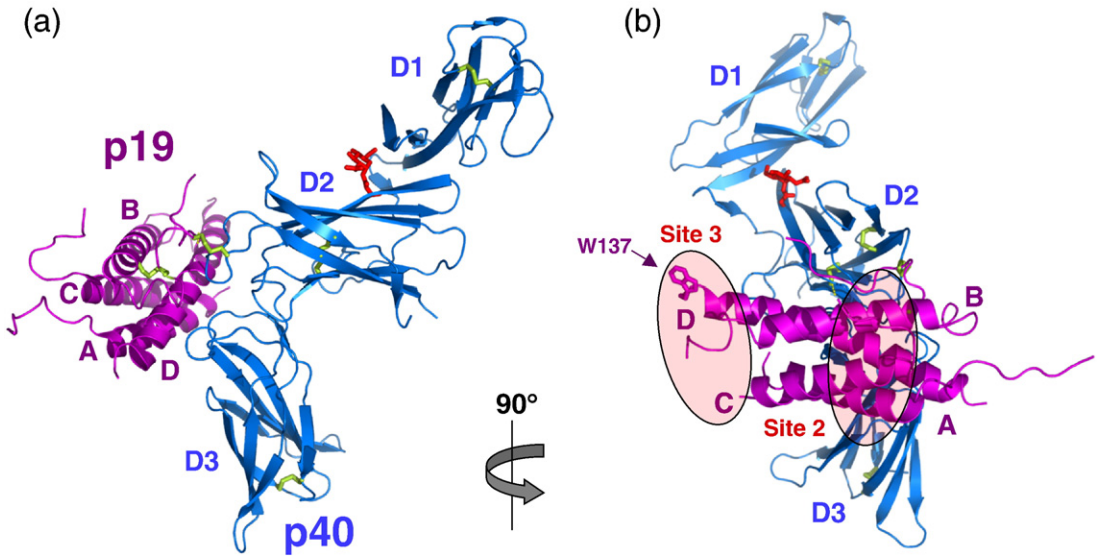

Fig. 2. Structure of IL-23. (a) Side view of the IL-23 crystal structure. p19 helices A to D are colored magenta, and p40 domains 1 to 3 are colored blue. The single *N*-acetylglucosamine residue attached to Asn200 on p40 is shown in red. Disulfide linkages are colored yellow. (b) Face-on view of IL-23. Receptor interaction sites 2 and 3 are highlighted in ovals, and the key site 3-interacting side chain of Trp137 is displayed.

nearly orthogonal orientation (Fig. 2b), as opposed to the more conventional end-to-end packing of tandem Ig domains, as seen for the D2 and D3 domains. The D2 and D3 domains represent the canonical cytokine-binding homology region found in all class I cytokine receptors, with the conserved disulfide bonds in D2 (C109–C120 and C148–C171). We observed one GlcNAc moiety emanating from Asn200 on the D2 domain that packs against the D1 domain but at a location distant from the cytokine binding site (Fig. 2). The remaining consensus Asn-linked glycosylation sites in p40 are unmodified or the glycans are disordered in the structure. The D3 domain contains the conserved WSXWS motif (WSEWA in p40) on the G strand. This consensus sequence is a part of a β-bulge and π-cation stacking motif in which side chains from the F strand (R287 and Q289) stack between aromatic residues on the WSEWA motif.

The four-helix bundle p19 is topologically similar to other canonical long-chain four-helix cytokines (Fig. 2a and b), which are, so far, the only known protein structures to exhibit an up–up–down–down helix topology. As is typical in cytokine structures, the helices are well ordered, while several inter-helical loops [residues 29–47 (A–B loop), 92–99 (B–C loop), and 123–137 (C–D loop)] lack defined electron density, which likely indicates flexibility of these regions. A comparison of p19 with all four-helix bundle cytokine structures shows the closest similarity with IL-6[24] (Dali *Z* score of 12.7 with an RMSD of 2.5 Å for 117 overlapping residues). p19 has ~15% sequence identity with p35, and superposition of 107 overlapping residues (out of 133) yields an RMSD of 2.3 Å (Dali *Z* score of 10.5). Thus, we speculate that even though both p19 and p35 engage p40, they are not simply paralogs of one another but may have undergone convergent evolution to engage p40 from distinct four-helix bundle precursors. The mature p19 polypeptide sequence is shorter than that of mature p35 by 27 residues, which is partially manifested in the structure by the truncation of the p19 A, C, and D helices by two, one, and two helical turns, respectively, compared to p35. A major deviation between the p19 and p35 structures is seen at the C-terminal end of the A–B loop in p35, which forms an 11-amino-acid disulfide-bonded loop (missing in p19) that forms two turns of an α-helix and forms numerous interactions with p40.

In the IL-23 interface, p40 loops 1 and 3 from the D2 domain and loops 5 and 6 from D3 interact with the p19 A and D helices, as well as the second half of the long A–B loop (Fig. 3a). The intersubunit disulfide bond unique to the IL-12/23 cytokines is formed at the top edge of the interface between p19 residue Cys54 on the A–B loop to p40 Cys177. This disulfide bond is peripheral to the main structural epitope between p19 and p40 and, in the case of IL-12, was shown not to be necessary for the p35/p40 interaction.[15] There is a large receptor–cytokine interface involving approximately 18 residues of p19 and 14 residues of p40 that buries 1730 Å^2 of surface area, with 830 Å^2 buried on p19 and 900 Å^2 buried on p40.

The p40 binding site forms a 'volcano-like' surface with Asp290 at the base of the crater, which is lined with hydrophobic residues such as Tyr246, Phe247, Tyr292, and Tyr293 (Fig. 3a). A peripheral group of both apolar and hydrogen-bonding residues (e.g., Arg208, Ser245, Glu181, and Arg291) forms a ring of 'peaks' surrounding the crater. In the heart of the interface, p19 extends Arg159 from its helix D into the crater such that its guanidium group forms an extensive network of interactions including a salt bridge to p40 residue Asp290 and a hydrogen bond to Tyr114. The ε-nitrogen of the p19 Arg159 guanidinium group also forms water-mediated hydrogen bonds to Tyr246 and Asp290 (Fig. 3a). These waters also hydrogen bond to the main chains of Ala179 of loop 3 and Ser248 of loop 5, respectively. There are several other ordered water molecules visible at the periphery of the interface that appear to stabilize the p40 interaction (Fig. 3b). In p40, the aromatic residues lining the crater of the 'arginine pocket' form multiple van der Waals interactions with backbone and side-chain atoms on helices A and D of p19 that surround the centrally protruding Arg159 (Fig. 3a). The principal interactions involve p40 Tyr292 packing against the p19 D helix main chain and forming hydrophobic contacts with p19 Ala155 and Ala158 and p40 Tyr293 interacting with p19 D helix Ala152 and A helix Trp26. The outermost shell of the interface exhibits several additional side-chain-specific hydrogen bonds from p40 residues Glu181 and Ser245, which interact with p19 residues His51 from the p19 A–B loop and His163, respectively (Fig. 3a). Collectively, the p19/p40 interface appears to have three shells of interactions: a charged center at the base of the crater, hydrophobic contacts lining the crater, and hydrogen-bonded peaks at the interface periphery. Thus, rather than the more conventional interface hotspot where a hydrophobic center is surrounded by polar periphery,[25,26] IL-23 has a polar center that appears insulated by a 'gasket' of hydrophobic interactions.

Although both p19 and p35 primarily use their A and D helices to engage p40, there are substantial positional changes with respect to the docking modes on p40. When the p40 molecules from both complexes are superimposed and the complexes are viewed looking down the barrels of the p19 and p35 four-helix bundles, it is clear that p19 is rotated clockwise towards the D2 domain of p40 by approximately 20° (Fig. 4a). When viewed from the top, p19 is also tilted towards p40 by approximately 10° compared to p35 (Fig. 4b). The overall result of the rotation and tilt of p19 with respect to p35 is that p19 has more intimate interaction between the N- and C-terminal ends of its D and A helices with p40 than with p35, and p35 has more intimate interactions with p40 at the C- and N-terminal ends of its D and A helices, respectively (Fig. 4b). In this latter region of the IL-12 interface, p40 loops 3 and 5 interdigitate into a 'corner' of p35 formed by an 11-amino-acid disulfide-bonded loop C-terminal to Cys74—this mini-loop is missing in

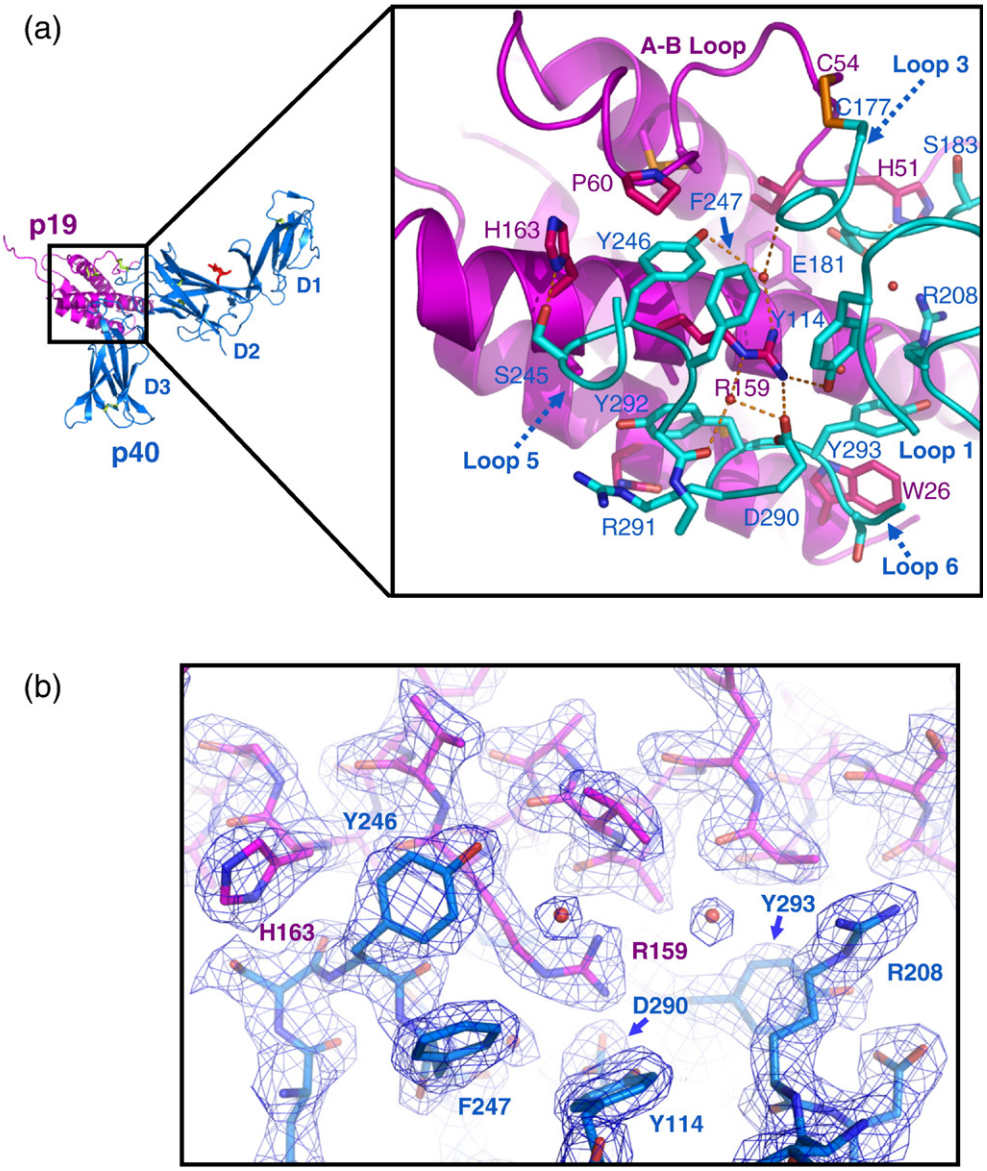

Fig. 3. Structural anatomy of the p19–p40 interface. (a) Close-up view of the secondary structure and amino acid contacts between p19 and p40. (b) Cutaway view of the arginine pocket $2F_o - F_c$ electron density contoured at 1.5 σ. Several well-ordered waters are visible at the interface, stabilizing the interaction of p40 pocket residues with Arg159.

p19. Thus, while p35 is less complementary with p40 at one end relative to p19, the rotation and tilt of the four-helix bundle results in improved complementarity at the opposite end.

In comparison to IL-12,[15] IL-23 has utilized the same network of charge and hydrogen bonds involving p40 residues Asp290 and Tyr114 at the base of the crater by structurally 'mimicking' the Arg189 on the D helix of p35 with its own p19 D helix Arg at position 159 (Fig. 4c). While a mutational analysis of interface residues was carried out for IL-12 to assess the energetic importance of p35/p40 contacts in complex assembly,[15] such data do not currently exist for IL-23. However, instructive comparisons can be made for obviously analogous structural contacts. In IL-12, residues that make up the hydrogen-bonding network involving the central Arg on the cytokine helix D, p40 residues Asp290 and Tyr114, are energetically critical as their mutation abrogates complex formation. We suggest that these residues in IL-23 are likely to be similarly energetically important. Given the vanishing sequence identity between p19 and p35, conservation of this core 'hotspot' in both complexes was unexpected. The positional correspondence of these residues (Fig. 4c) and their interactions in the face of highly divergent sequence and docking positions on p40 further suggests convergent structural evolution from distinct precursors to recapitulate the features of this 'arginine' pocket in both heterodimers. The hydrogen bonds in the arginine pocket in the two complexes are not exactly similar, most likely due to a slight shift in backbone position of the p19 Arg159 *versus* p35 Arg189, which affects the side-chain location and geometry of the resultant bonding network (Fig. 4c). Further, direct comparisons of the

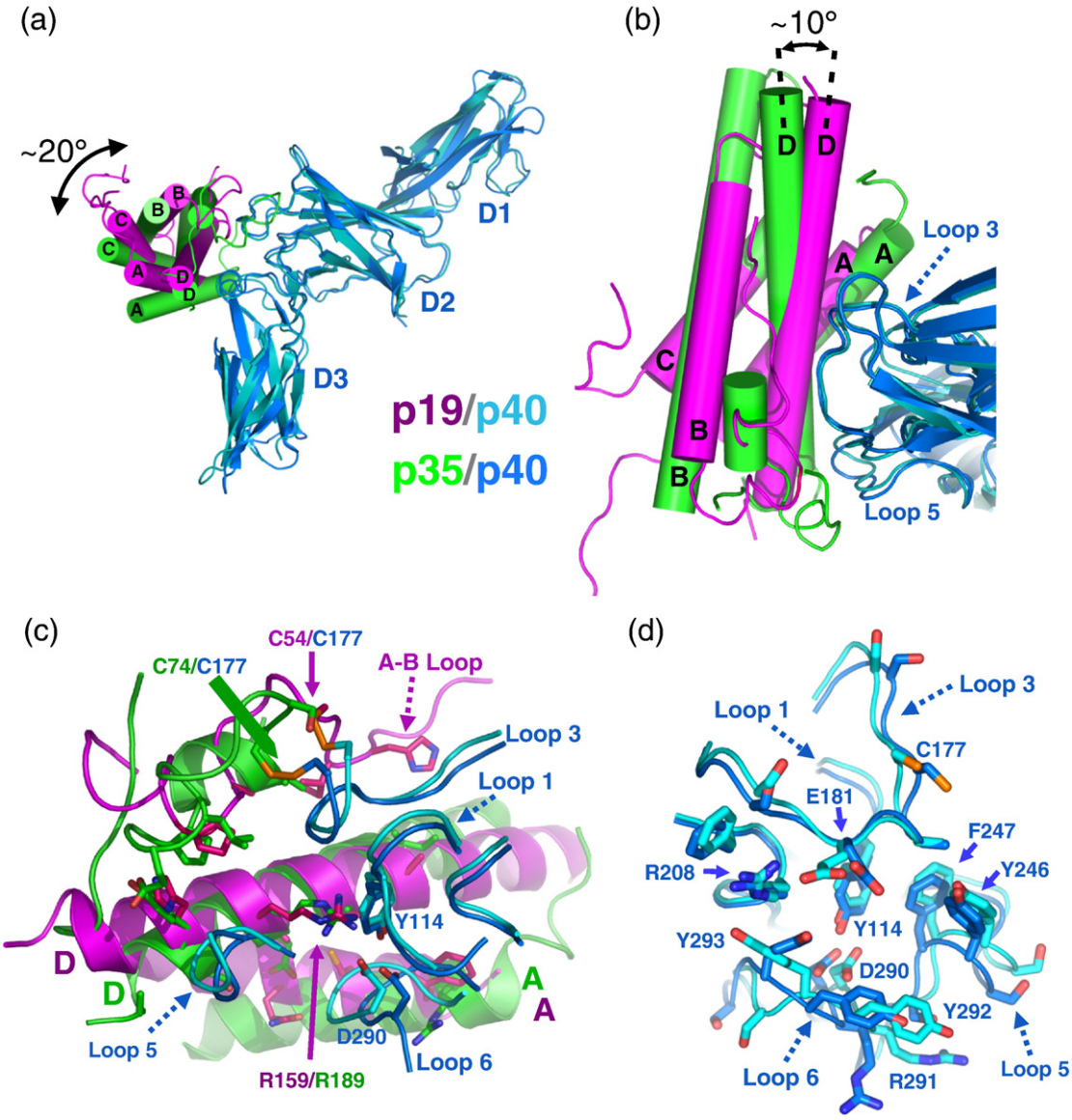

Fig. 4. Comparative analysis of IL-23 and IL-12. (a) p19 (pink) is 'rolled' towards the D2 of p40 (blue) by ~20° and (b) tilted by ~10° when compared to p35 (green). (c) Overlay of the p19–p40 and p35–p40 interaction interfaces when p40 is structurally superimposed. Note the intact side-chain positioning of p19 Asp159 and p40 arginine pocket residues. All contact residues on p19 and p35 are drawn as sticks. (d) Comparison of the four-helix bundle interacting loops of p40 from the two structures (IL-23 p40 in cyan and IL-12 p40 in blue) reveals only slight distortions in the positioning of the loops when bound to their respective four-helix cytokines.

role of bound water molecules in the respective interfaces are complicated by the differing resolutions of the structures (IL-23, 2.3 Å *versus* IL-12, 2.8 Å). Nevertheless, it is clear that the interactions that form the arginine pocket are structurally conserved and, therefore, likely to be important for heterodimer formation in both cytokines.

The surrounding interactions in the IL-23 and IL-12 interfaces, however, are almost entirely different (Table 2), which was to be expected given the limited sequence identity between p19 and p35. Comparison of the two interfaces reveals that, with the exception of the central arginine residue discussed above, there are no other conserved pairwise interactions (Table 2). Many of the same p40 residues are buried within the different interfaces (Fig. 5a) and serve similar structural roles in both complexes but through interactions with distinct constellations of amino acids on the p19 and p35 surfaces (Fig. 5b). For instance, in the interface 'outer shell,' p40 residue Glu181, which was shown in IL-12 to be energetically critical for heterodimer formation,[15] forms a hydrogen bond with Arg183 in p35 *versus* His51 in p19. Ser245 of p40, whose mutation to Ala had a modest effect in the IL-12 system, hydrogen bonds to the amide nitrogen of Tyr193 in p35 *versus* the side chain of His163 in p19. In the IL-23 complex, p40 forms several more interactions with the p19 A–B loop near the Cys54–Cys177 interchain disulfide linkage (Fig. 3c), which may be a result of the rotation of p19 towards p40 relative to p35. In IL-12, the A–B loop is largely disordered with the

Table 2. Shared and distinct contacts between p40 and the four-helix bundles p19 and p35

p40 residue	p19 residue	vdW[a]	H-bonds[b]	p35 residue	vdW[a]	H-bonds[b]
Tyr114	Arg159	1	1	Arg189	4	1
Ser175		0	0	Ser73	3	0
Ala176		0	0	Ser73	2	0
Cys177	Cys54	4	0	Ser73	6	0
				Cys74		
Pro178		0	0	Cys74	1	0
Ala179	Asp59	2	0	Val60	3	0
	Val156			Leu68		
Ala180	Ile52	2	0		0	0
Glu181	His51	18	3	Ile182	11	3
	Ile52			Arg183		
	Phe153			Thr186		
Ser183	His51	1	0		0	0
Arg208	Ala152	4	0	Ile182	3	0
Thr242		0	0	Leu68	1	0
Pro243	His163	1	0	Glu67	4	0
Ser245	Ala162	6	1	Ser192	11	1
	His163			Tyr193		
	Thr167			Ala196		
Tyr246	Cys58	15	1	Pro65	9	1
	Pro60			Arg189		
	Arg159					
	His163					
Phe247		0	0	Arg189	2	0
Ser248		0	0	Ser192	1	0
Gln289		0	0	Arg34	2	0
Asp290	Arg159	1	2	Arg34	2	1
Arg291		0	0	Arg34	2	0
Tyr292	Gln19	17	0	Arg34	16	2
	Cys22			Arg181		
	Ala155			Asp188		
	Ala158			Arg189		
	Arg159					
	Ala162					
Tyr293	Trp26	6	0	Arg34	15	1
	Ala152			Arg181		
				Ile182		
				Val185		
Ser294	Trp26	8	0	Arg34	1	1
Ser295		0	0	Arg34	1	0

Yellow shaded residues in p40 column are shared by p19 and p35, while green and purple shaded residues are ligand specific contacts. (For interpretation of the references to colour in this table legend, the reader is referred to the web version of this article.)

[a] van der Waals cutoff distance of 3.9 Å.

[b] Hydrogen bond cutoff distance of 3.5 Å.

exception of residues C-terminal to the p35 Cys74, and this disorder may be a result of the gap between p35 and p40 above the D helix, formed by the relative rotation of p35 away from p40. Collectively, p40 displays an ability to engage two different cytokine surfaces through a combination of shared (Arg pocket) and distinct interactions (outer shells).

The cross-reactivity of p40 is not due to large-scale conformational changes in the binding site. Superposition of p40 from both heterodimers reveals that the backbone conformations of the p40 loops are generally similar, although several of the loops are slightly distorted (Fig. 4d). We interpret this as small-scale structural accommodation of the different p19 and p35 cytokine surfaces by somewhat malleable, solvent-exposed p40 loops, as has been previously reported for receptor–cytokine interactions in the gp130 and IL-4/13 receptor systems,[26,27] rather than an 'induced fit' binding mechanism in which distinct loop conformations adapt to the divergent surfaces. Strikingly, the center of the arginine pocket, including residues Asp290, Tyr114, and Phe247 of p40, has preserved their side-chain and main-chain positions in the two complexes (Fig. 4d). These residues, including Phe247, are energetically essential for formation of the IL-12 complex.[15] The main conformational deviations seen in the p40 binding site are localized to loop 6 of the p40 D3 domain, where Arg291, Tyr292, and Tyr293 assume different side-chain positions. It therefore appears that p40 has preserved the structural context of most of the energetically critical residues used in the IL-12 heterodimer that are also in contact with p19, further supporting their conserved role in IL-23.

To further investigate the basis for the cross-reactivity of p40 for p19 and p35, we analyzed the interchain contacts and buried surface area for each p40 residue that makes contact with either p19 or p35 (Table 2 and Fig. 5a). Clearly, p40 uses the same binding surface to contact both p19 and p35 (Fig. 5b - middle). However, when analyzed in terms

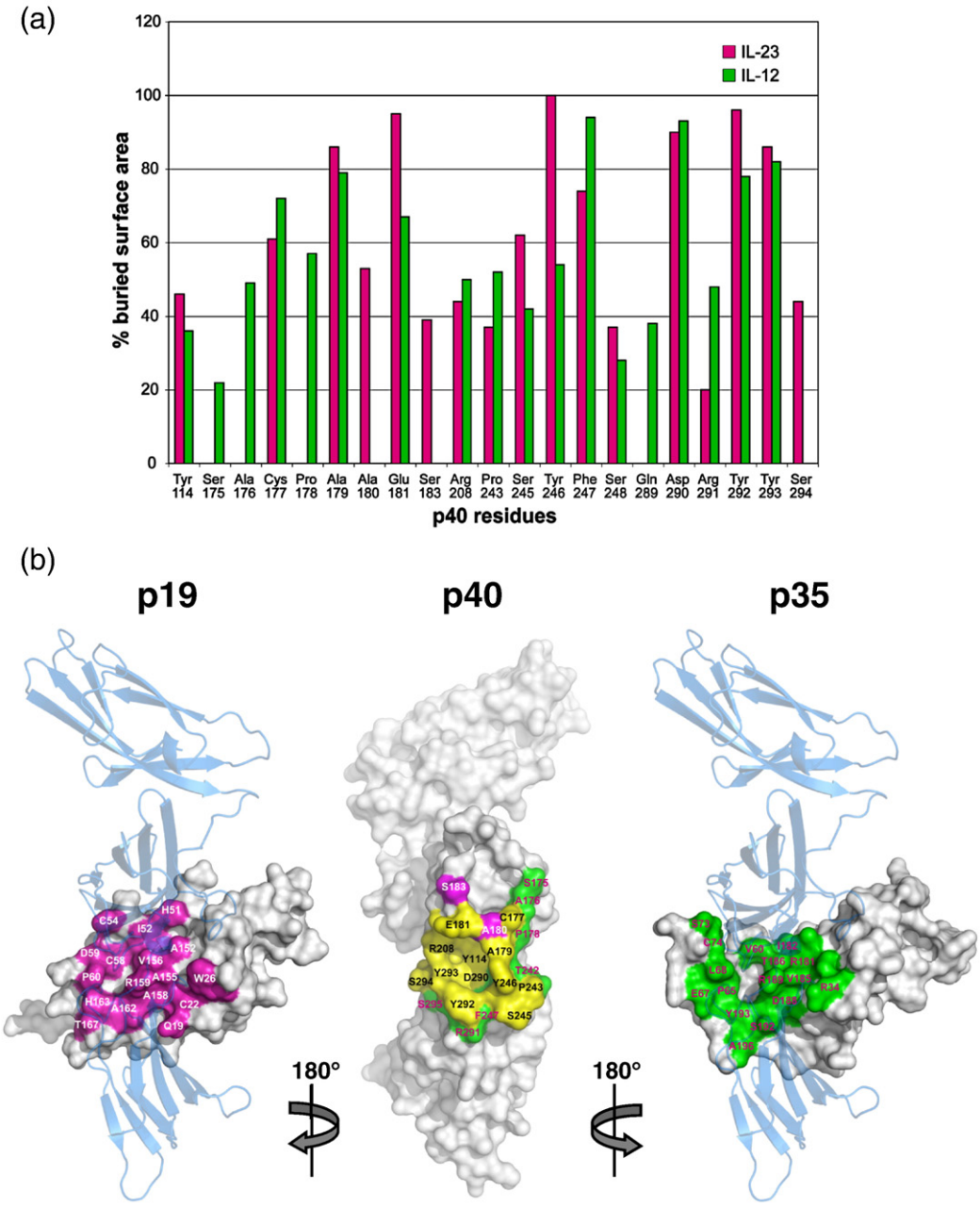

Fig. 5. Comparison of shared and distinct contact surfaces in the IL-23 and IL-12 complexes. (a) Histogram of buried surface area contributed by each p40 residue involved in p19 and/or p35 interaction. (b) Surface representation of p40 (middle panel), with residues interacting with p19 (pink), p35 (green), or p19 and p35 (yellow) highlighted. The p40-interacting surfaces of p19 (left panel in pink) and p35 (right panel in green) are shown with a transparent p40 overlay to demonstrate orientation.

of interatomic contacts (Table 1 and Fig. 5a) of the 23 total p40 residues that make contact with either cytokine, we find that 12 (~1/2) of these residues are shared contact residues. Nine of the remaining residues only contact p35, while 2 only contact p19. The bulk of this disparity reflects the added contact area provided by the A–B loop extension found in p35. The two amino acids that exclusively contact p19 are found at the C-terminal end of loop 3 in p40 and interact with p19 in the ordered section of the A–B loop around the interchain disulfide at Cys54 (discussed earlier). These data are represented graphically in Fig. 5b, with shared residues on the surface representation of p40 (middle panel) colored yellow and p19- and p35-exclusive residues colored pink and green, respectively (Table 2 is colored similarly).

Discussion

As both IL-12 and IL-23 are attractive therapeutic targets for various autoimmune diseases, one goal is to develop small-molecule inhibitors of heterodimer formation.[15] Small-molecule antagonism of

cytokine–receptor interactions remains a daunting, but important, challenge given how important many cytokine–receptor interactions are in human health and disease. While antibodies can be highly effective antagonists, production costs are high and special storage and handling are required. Despite the immense difficulties in producing small-molecule antagonists of protein–protein interactions, one notable exception has been the four-helix cytokine IL-2, for which a panel of high-affinity small molecules that antagonize its association with its α-receptor has been created.[28] Comparison of the IL-2/drug and IL-2/IL-2Rα complexes revealed that the drug utilizes a similar binding epitope on the cytokine as the receptor.[29] Further, an alanine scanning study showed that the drug uses the same energetic hotspots on IL-2 as the receptor, despite inducing conformational changes on the cytokine surface.[30] Given this encouraging proof of concept, small-molecule targeting of cytokines remains an active effort in the pharmaceutical industry.

Due to the different activities of IL-12 and IL-23 on Th1 and Th17 responses, respectively, the ultimate therapeutic goal would likely be to target one cytokine specifically in order to modulate these responses independently. The shared use of p40 by these cytokines would presumably make it difficult to develop drugs against p40 that target one heterodimer *versus* the other. Our comparative structural analysis of the p19 and p35 interfaces with p40 reveals that the majority of the helical cytokine surfaces involved in p40 interactions are structurally unique and cross-reactivity of a drug targeted against p19 or p35 would be unlikely. On the other hand, the majority of p40 residues contacting p19 also contact p35, rendering p40 a more difficult target for design of a cytokine-specific antagonist. However, the p40 binding surfaces are not entirely redundant, and in fact, several residues are used specifically in p19 or p35 interactions (Table 2 and Fig. 5b). For example, p40 residues Ala180 and Ser183 only contact p19, whereas approximately nine p40 residues are used only for p35 contact. Most of these latter residues are on the p40 loops 5 and 6, which have extensive contact with the p35 disulfide-bonded mini-loop that is not present in p19. Therefore, we conclude that there are sufficient structural differences in these interfaces that, in principle, a small molecule or antibody could selectively interfere with formation of IL-12 or IL-23 by targeting either the cytokines or p40.

The IL-23 heterodimer engages the signaling receptors IL-12Rβ1 and IL-23R in order to induce a cellular response via the Jak/Stat pathway (Fig. 1). Previous structural studies in the gp130 system provide an architectural template to model the IL-23 quaternary complex.[6,26,31] Cytokines of the gp130 family possess a 'site III' at the tip of the cytokine that engages an Ig domain on one of the signaling receptors, in addition to canonical sites I and II on each side of the four-helix bundle. In the p19 structure, the loop connecting the C–D helices contains a tryptophan (Trp137) residue that is a signature hallmark of the site III interaction (Fig. 2b), as is also seen in members of the gp130 cytokine family.[6,31] For IL-23, the p19/p40 heterodimer represents the site I complex. Given that IL-12Rβ1 does not possess an Ig domain, the only possible site it could engage on IL-23 would be site II (Fig. 2b), binding the A and B helices of p19 in an orientation similar to the manner in which IL-6 engages gp130. This would leave the tip of p19 available to engage the Ig domain of IL-23R to form a quaternary signaling complex. By analogy, the p35/p40 heterodimer would also engage IL-2Rβ1 at site II and recruit the Ig domain containing IL-12Rβ2 to site III to similarly form a quaternary complex (Fig. 1). Future structural studies will clarify the assembly pathways and molecular architecture of the IL-23 and IL-12 signaling complexes and will likely reveal additional targets of opportunity for structure-based design of antagonists.

Materials and Methods

Protein expression and purification

Recombinant IL-23 used for crystallization was expressed using the baculovirus system. High-titer baculovirus stocks were prepared by transfection and amplification in *Spodoptera frugiperda* (SF9) cells cultured at 28 °C in SF900 II media (Invitrogen). Protein expression was carried out in *Trichoplusia ni* (Hi-Five, Invitrogen) cells growing in suspension in Insect Xpress media (Lonza).

Human p19 (residues 20–189) and p40 (residues 23–328) cDNAs were cloned into the insect cell expression vector pACSG2 (BD Biosciences) in frame with an N-terminal gp67 leader sequence and C-terminal hexahistidine tag. To generate glycan-minimized IL-23, we coinfected kifunensine-treated Hi-Five cells with p19 and p40 viruses along with virus carrying the endoglycosidase-H (endoH) cDNA and we allowed protein to express for 48 h. The p19/p40 IL-23 heterocomplex was captured from supernatant using Ni-agarose (Qiagen) with yields approaching 20 mg/L. Ni-purified IL-23 was diluted to 1 mg/mL, subjected to reductive methylation,[32] concentrated, and purified by fast protein liquid chromatography on a Superdex 200 16/60 size-exclusion column (GE Healthcare) equilibrated in 10 mM Hepes, pH 7.0, and 150 mM NaCl. Peak fractions were pooled and concentrated for crystallization.

Crystallization and data collection

Initial crystallization trials yielded small triangular platelike crystals from the Peg-Ion crystallization screen (Hampton Research) using the sitting drop method at 25 °C. Ultimately, diffraction-quality crystals were grown in sitting drops at 25 °C by mixing 0.5 μL of protein (15 mg/mL in 10 mM Hepes-NaOH, pH 7.0, and 150 mM NaCl) with an equal volume of 0.1 M Hepes-NaOH, pH 7.0, 20% polyethylene glycol 3350, and 0.2 M potassium nitrate. Crystals grew to maximum dimensions of 300 μm × 300 μm × 100 μm in 1–2 weeks. Crystals were flash frozen in liquid nitrogen using mother liquor containing 25% v/v glycerol as a cryoprotectant, and a 2.3-Å data set was collected under cryo-cooled conditions at beamline 11-1 at the Stanford Synchotron Radiation

Laboratory. Diffraction data were processed using MOSFLM[33] and SCALA.[34] Data processing statistics can be found in Table 2.

Structure determination and refinement

Initial phase information was obtained with the program Phaser[36] using the p40 subunit from the IL-12 structure [Protein Data Bank (PDB) ID 1F45] as a molecular replacement search model. After initial refinement of the molecular replacement solution, the α-helices of p19 were visible and could be built into the electron density map using Coot.[37] The model was refined by iterative rounds of simulated annealing, positional minimization, and *B*-factor refinement using CNS[38] followed by model adjustment with Coot. The final model went through restrained refinement using REFMAC,[39] resulting in a final R_{work} and R_{free} of 22.8% and 26.8%, respectively. Ramachandran analysis by PROCHECK[35] indicates that 87.1% of residues reside in the most favorable regions, 12.8% in additionally allowed regions, and two residues (K95 in each p40 chain) in the disallowed region. All structural figures were prepared using PyMOL†. Contact and buried surface area were calculated with the CCP4 program suite[34] and the Protein Interfaces, Surfaces and Assemblies server‡.

The final model contains two copies of IL-23 in the asymmetric unit, with p40 chain A and p19 chain C making up one copy and p40 chain B and p19 chain D making up the other copy. p40 chain A consists of amino acids 1–156 and 164–306, with two loops modeled mostly as alanines (residues 99–100, 102–104, 258–260, and 262–263). p40 chain B consists of amino acids 1–156, 162–224, 229–258, and 263–305, with one loop modeled mostly as alanines (99–100 and 102–104) and alanines at positions 258 and 263. p19 chain C consists of amino acids 1–29, 47–94, 100–125, and 137–169, with alanines modeled at positions 29 and 47–48. p19 chain D consists of amino acids 1–28, 47–91, 97–122, and 137–170, with three histidine residues modeled at the C-terminus. A single *N*-acetylglucosamine moiety is found in each p40 chain attached to Asp200. The amino acid numbering scheme used corresponds to the mature protein chain with the signal peptide cleaved, in order to facilitate comparison between IL-12 and IL-23. Additionally, all four chains have one to two amino acids from the gp67 signal sequence modeled at their N-termini, with the mature protein sequence starting at position 1.

PDB accession code

The atomic coordinates and structure factors for IL-23 have been deposited in the PDB under accession code 3DUH.

Acknowledgements

We thank Sean Juo for assistance with data collection, structure analysis, and helpful discussion of the manuscript. We thank Rob Kastelein and Fernando Bazan for helpful discussions. P.J.L. is a Damon Runyon Fellow, supported by the Damon Runyon Cancer Research Foundation (DRG-1928-06). This work was funded by National Institutes of Health grant (AI51321) and a Sandler Program in Asthma Research (SPAR) grant to K.C.G. K.C.G. is also supported by the Keck Foundation and the Howard Hughes Medical Institute.

† http://www.pymol.org

‡ http://www.ebi.ac.uk/msd-srv/prot_int/pistart.html

References

1. Leonard, W. J. & O'Shea, J. J. (1998). Jaks and STATs: biological implications. *Annu. Rev. Immunol.* **16**, 293–322.
2. Sprang, S. R. & Bazan, J. F. (1993). Cytokine structural taxonomy and mechanisms of receptor engagement. *Curr. Opin. Struct. Biol.* **3**, 815–827.
3. Bazan, J. F. (1990). Structural design and molecular evolution of a cytokine receptor superfamily. *Proc. Natl. Acad. Sci. USA*, **87**, 6934–6938.
4. de Vos, A. M., Ultsch, M. & Kossiakoff, A. A. (1992). Human growth hormone and extracellular domain of its receptor: crystal structure of the complex. *Science*, **255**, 306–312.
5. Wells, J. A. & de Vos, A. M. (1996). Hematopoietic receptor complexes. *Annu. Rev. Biochem.* **65**, 609–634.
6. Chow, D., He, X., Snow, A. L., Rose-John, S. & Garcia, K. C. (2001). Structure of an extracellular gp130 cytokine receptor signaling complex. *Science*, **291**, 2150–2155.
7. Boulanger, M. J. & Garcia, K. C. (2004). Shared cytokine signaling receptors: structural insights from the gp130 system. *Adv. Protein Chem.* **68**, 107–146.
8. Parham, C., Chirica, M., Timans, J., Vaisberg, E., Travis, M., Cheung, J. *et al.* (2002). A receptor for the heterodimeric cytokine IL-23 is composed of IL-12Rbeta1 and a novel cytokine receptor subunit, IL-23R. *J. Immunol.* **168**, 5699–5708.
9. Pflanz, S., Hibbert, L., Mattson, J., Rosales, R., Vaisberg, E., Bazan, J. F. *et al.* (2004). WSX-1 and glycoprotein 130 constitute a signal-transducing receptor for IL-27. *J. Immunol.* **172**, 2225–2231.
10. Trinchieri, G., Pflanz, S. & Kastelein, R. (2003). The IL-12 family of heterodimeric cytokines: new players in the regulation of T-cell responses. *Immunity*, **19**, 641–644.
11. Kastelein, R. A., Hunter, C. A. & Cua, D. J. (2007). Discovery and biology of IL-23 and IL-27: related but functionally distinct regulators of inflammation. *Annu. Rev. Immunol.* **25**, 221–242.
12. Oppmann, B., Lesley, R., Blom, B., Timans, J. C., Xu, Y., Hunte, B. *et al.* (2000). Novel p19 protein engages IL-12p40 to form a cytokine, IL-23, with biological activities similar as well as distinct from IL-12. *Immunity*, **13**, 715–725.
13. Gubler, U., Chua, A. O., Schoenhaut, D. S., Dwyer, C. M., McComas, W., Motyka, R. *et al.* (1991). Coexpression of two distinct genes is required to generate secreted bioactive cytotoxic lymphocyte maturation factor. *Proc. Natl. Acad. Sci. USA*, **88**, 4143–4147.
14. Wolf, S. F., Temple, P. A., Kobayashi, M., Young, D., Dicig, M., Lowe, L. *et al.* (1991). Cloning of cDNA for natural killer cell stimulatory factor, a heterodimeric cytokine with multiple biologic effects on T and natural killer cells. *J. Immunol.* **146**, 3074–3081.
15. Yoon, C., Johnston, S. C., Tang, J., Stahl, M., Tobin, J. F. & Somers, W. S. (2000). Charged residues dominate a unique interlocking topography in the heterodimeric cytokine interleukin-12. *EMBO J.* **19**, 3530–3541.

16. Briso, E. M., Dienz, O. & Rincon, M. (2008). Cutting edge: soluble IL-6R is produced by IL-6R ectodomain shedding in activated CD4 T cells. *J. Immunol.* **180**, 7102–7106.
17. Presky, D. H., Yang, H., Minetti, L. J., Chua, A. O., Nabavi, N., Wu, C. Y. *et al.* (1996). A functional interleukin 12 receptor complex is composed of two beta-type cytokine receptor subunits. *Proc. Natl. Acad. Sci. USA*, **93**, 14002–14007.
18. Huyton, T., Zhang, J. G., Luo, C. S., Lou, M. Z., Hilton, D. J., Nicola, N. A. & Garrett, T. P. (2007). An unusual cytokine:Ig-domain interaction revealed in the crystal structure of leukemia inhibitory factor (LIF) in complex with the LIF receptor. *Proc. Natl. Acad. Sci. USA*, **104**, 12737–12742.
19. Aggarwal, S., Ghilardi, N., Xie, M. H., de Sauvage, F. J. & Gurney, A. L. (2003). Interleukin-23 promotes a distinct CD4 T cell activation state characterized by the production of interleukin-17. *J. Biol. Chem.* **278**, 1910–1914.
20. Yen, D., Cheung, J., Scheerens, H., Poulet, F., McClanahan, T., McKenzie, B. *et al.* (2006). IL-23 is essential for T cell-mediated colitis and promotes inflammation via IL-17 and IL-6. *J. Clin. Invest.* **116**, 1310–1316.
21. Murphy, C. A., Langrish, C. L., Chen, Y., Blumenschein, W., McClanahan, T., Kastelein, R. A. *et al.* (2003). Divergent pro- and antiinflammatory roles for IL-23 and IL-12 in joint autoimmune inflammation. *J. Exp. Med.* **198**, 1951–1957.
22. Langrish, C. L., Chen, Y., Blumenschein, W. M., Mattson, J., Basham, B., Sedgwick, J. D. *et al.* (2005). IL-23 drives a pathogenic T cell population that induces autoimmune inflammation. *J. Exp. Med.* **201**, 233–240.
23. Langowski, J. L., Zhang, X., Wu, L., Mattson, J. D., Chen, T., Smith, K. *et al.* (2006). IL-23 promotes tumour incidence and growth. *Nature*, **442**, 461–465.
24. Somers, W., Stahl, M. & Seehra, J. S. (1997). 1.9 Å crystal structure of interleukin 6: implications for a novel mode of receptor dimerization and signaling. *EMBO J.* **16**, 989–997.
25. Clackson, T. & Wells, J. A. (1995). A hot spot of binding energy in a hormone–receptor interface. *Science*, **267**, 383–386.
26. Boulanger, M. J., Bankovich, A. J., Kortemme, T., Baker, D. & Garcia, K. C. (2003). Convergent mechanisms for recognition of divergent cytokines by the shared signaling receptor gp130. *Mol. Cell*, **12**, 577–589.
27. LaPorte, S. L., Juo, Z. S., Vaclavikova, J., Colf, L. A., Qi, X., Heller, N. M. *et al.* (2008). Molecular and structural basis of cytokine receptor pleiotropy in the interleukin-4/13 system. *Cell*, **132**, 259–272.
28. Thanos, C. D., Randal, M. & Wells, J. A. (2003). Potent small-molecule binding to a dynamic hot spot on IL-2. *J. Am. Chem. Soc.* **125**, 15280–15281.
29. Rickert, M., Wang, X., Boulanger, M. J., Goriatcheva, N. & Garcia, K. C. (2005). The structure of interleukin-2 complexed with its alpha receptor. *Science*, **308**, 1477–1480.
30. Thanos, C. D., DeLano, W. L. & Wells, J. A. (2006). Hot-spot mimicry of a cytokine receptor by a small molecule. *Proc. Natl. Acad. Sci. USA*, **103**, 15422–15427.
31. Boulanger, M. J., Chow, D. C., Brevnova, E. E. & Garcia, K. C. (2003). Hexameric structure and assembly of the interleukin-6/IL-6 alpha-receptor/gp130 complex. *Science*, **300**, 2101–2104.
32. Walter, T. S., Meier, C., Assenberg, R., Au, K. F., Ren, J., Verma, A. *et al.* (2006). Lysine methylation as a routine rescue strategy for protein crystallization. *Structure*, **14**, 1617–1622.
33. Leslie, A. G. W. (1992). Recent changes to the MOSFLM package for processing film and image plate data. *Joint CCP4+ESF-EAMCB Newsletter on Protein Crystallography*, **26**.
34. Potterton, E., Briggs, P., Turkenburg, M. & Dodson, E. (2003). A graphical user interface to the CCP4 program suite. *Acta Crystallogr., Sect. D: Biol. Crystallogr.* **59**, 1131–1137.
35. Laskowski, R. A., MacArthur, M. W., Moss, D. S. & Thornton, J. M. (1993). PROCHECK: a program to check the stereochemical quality of a protein structure. *J. Appl. Crystallogr.* **26**, 283.
36. McCoy, A. J., Grosse-Kunstleve, R. W., Adams, P. D., Winn, M. D., Storoni, L. C. & Read, R. J. (2007). Phaser crystallographic software. *J. Appl. Crystallogr.* **40**, 658–674.
37. Emsley, P. & Cowtan, K. (2004). Coot: model-building tools for molecular graphics. *Acta Crystallogr., Sect. D: Biol. Crystallogr.* **60**, 2126–2132.
38. Brunger, A. T. (2007). Version 1.2 of the crystallography and NMR system. *Nat. Protoc.* **2**, 2728–2733.
39. Murshudov, G. N., Vagin, A. A. & Dodson, E. J. (1997). Refinement of macromolecular structures by the maximum-likelihood method. *Acta Crystallogr., Sect. D: Biol. Crystallogr.* **53**, 240–255.